biology letters

Biol. Lett. (2008) **4**, 430–433
doi:10.1098/rsbl.2008.0166
Published online 29 May 2008

Population genetics

A coalescent framework for comparing alternative models of population structure with genetic data: evolution of Celebes toads

Ben J. Evans[1,*], Jimmy A. McGuire[2], Rafe M. Brown[3], Noviar Andayani[4] and Jatna Supriatna[4]

[1]*Department of Biology, Life Sciences Building Room 328, McMaster University, 1280 Main Street West, Hamilton, Ont., Canada L8S 4K1*
[2]*Department of Integrative Biology, 3101 Valley Life Sciences Building, University of California, Berkeley, CA 94720-3160, USA*
[3]*Department of Ecology and Evolutionary Biology, Dyche Hall, University of Kansas, 1345 Jayhawk Boulevard, Lawrence, KS 66045-7561, USA*
[4]*Departmen Biologi, FMIPA, University of Indonesia, Depok, Java 16424, Indonesia*
**Author for correspondence* (evansb@mcmaster.ca).

Isolation of populations eventually leads to divergence by genetic drift, but if connectivity varies over time, its impact on diversification may be difficult to discern. Even when the habitat patches of multiple species overlap, differences in their demographic parameters, molecular evolution and stochastic events contribute to differences in the magnitude and distribution of their genetic variation. The Indonesian island of Sulawesi, for example, harbours a suite of endemic species whose intraspecific differentiation or interspecific divergence may have been catalysed by habitat fragmentation. To further test this hypothesis, we have performed phylogenetic and coalescent-based analyses on molecular variation in mitochondrial and nuclear DNA of the Celebes toad (*Bufo celebensis*). Results support a role for habitat fragmentation that led to a population structure in these toads that closely matches distributions of Sulawesi macaque monkeys. Habitat fragmentation, therefore, may also have affected other groups on this island.

Keywords: coalescence; rejection sampling; demography

1. INTRODUCTION

Fragmentation of populations can cause divergence by genetic drift depending on their effective population sizes, mutation rate, the duration of isolation, and the level of gene flow between them. However, the role of fragmentation in causing population structure may be subtle after what we call ‘cryptic fragmentation’, in which a barrier to gene flow is either not apparent or no longer present. Cryptic fragmentation may have affected, for example, fauna of the island of Cuba (Glor *et al.* 2004) and the Baja California Peninsula (Leaché *et al.* 2007). In contrast to diversification caused by enduring barriers to dispersal, the genetic signature of cryptic fragmentation might fade over time if the margins of the subdivided populations move, or if recent gene flow causes populations to amalgamate.

Cryptic fragmentation has been proposed on the Indonesian island of Sulawesi based on similar patterns of diversity in multiple groups, including the Celebes toad (Evans *et al.* 2003*c*), monkeys (Evans *et al.* 2003*b*), fanged frogs (Evans *et al.* 2003*a*) and flying lizards (McGuire *et al.* 2007). However, the validity of a demographic model of isolation by distance (IBD) plus fragmentation as opposed to a model of exclusively IBD has been questioned (Bridle *et al.* 2004). To further explore this, we used a coalescent-based approach to compare the fit of models that approximate each of these demographic scenarios for the Celebes toad, *Bufo celebensis*.

2. MATERIAL AND METHODS

(a) *Molecular data, genealogies, networks and population subdivision*

New data were collected from mitochondrial DNA (mtDNA) and two nuclear loci (nDNA) from throughout the range of the Celebes toad, including sequences from up to 166 individual toads from up to 56 localities (figures 1*a* and 2*a*; see the electronic supplementary material). MtDNA sequences are from the 12S rDNA gene and nuclear sequences are from the recombination activation gene 1 (*RAG*) and intron 3 of the rhodopsin gene (*RHO*). A phylogeny was estimated from the mtDNA data under a doublet model for ribosomal genes using MrBayes v. 3.1.2 (Huelsenbeck & Ronquist 2001) with secondary structure inferred from a model for *Xenopus laevis* (Cannone *et al.* 2002). Networks were estimated from inferred alleles for the nuclear loci (see the electronic supplementary material).

(b) *Coalescent comparison of alternative demographic models*

For computational efficiency (Wilkins 2004), we used a lattice model to approximate an IBD model (IBD_L), and compared it with an alternative model that also has simultaneous fragmentation (IBD_L+F) at the sites of each macaque contact zone, except a displaced location of the margin in toads between the NW and WC areas of endemism (AOEs; figure 2*a*). The locations of macaque contact zones are well characterized (Evans *et al.* 2003*b* and references therein). Both models assume mutation–drift equilibrium, constant population size over time and symmetrical migration between connected neighbouring demes.

The IBD_L model has three parameters: the effective population size of the locus in each deme ($N_{e\text{-nDNA-deme}}$), the mutation rate per sequence (μ) and the fraction of subpopulation i in each generation that are migrants from subpopulation j (m_{ij}). The IBD_L+F model has an additional parameter (τ), which is the time in $4N_{e\text{-nDNA-deme}}$ generations from the present that fragmentation started simultaneously at all boundaries between AOEs (figure 2*a*).

Model likelihood was estimated using rejection sampling of coalescent simulations (Weiss & von Haeseler 1998) based on three summary statistics: the average pairwise nucleotide divergence per sequence (π), the number of segregating sites (S) and F_{ST} (table 1). π and S were calculated for simulated data using sample_stat (Hudson 2002) and for the observed data using DnaSP v. 4.10.9 (Rozas *et al.* 2003). F_{ST} was calculated using Perl scripts according to: $F_{ST}=(\pi_{between}-\pi_{within})/\pi_{between}$ where $\pi_{between}$ and π_{within} are the average number of pairwise differences between and within AOEs, respectively (Hudson *et al.* 1992). To avoid bias due to differences in sample size, the average π_{within} of each AOE was used in this calculation. F_{ST} was transformed according to $F_{ST}/(1-F_{ST})$ (Rousset 1997) before rejection sampling. Model likelihood for each locus was estimated as the proportion of 100 000 simulations whose summary statistics were $\pm 10\%$ of the observed values for all three statistics; multilocus likelihoods are the product of the likelihood of each locus. Simulations were performed with the program ms (Hudson 2002) under an approximation of the finite sites model by using the total mutation rate for each sequence instead of the mutation rate per site, which is appropriate when $4N_e\mu$/site is small. Scaling factors were applied to $N_{e\text{-nDNA-deme}}$ and μ as a coarse measure to accommodate

Electronic supplementary material is available at http://dx.doi.org/10.1098/rsbl.2008.0166 or via http://journals.royalsociety.org.

Received 23 March 2008
Accepted 14 May 2008

Table 1. Polymorphism statistics for sequence data from the Celebes toad for mtDNA, *RAG* and *RHO*. (The number of unique haplotypes (no.) on Sulawesi (all) and each area of endemism (AOE) are indicated, with labelling of AOEs following figure 1. Other statistics (π, S and F_{ST}) are discussed in the text.)

	mtDNA	*RAG*	*RHO*
base pairs	727	961	338
S	80	21	10
π per site	0.03144	0.00254	0.00379
π per sequence	22.85688	2.44094	1.28102
F_{ST}	0.91460	0.46068	0.46469
no. all	32	22	15
no. NE AOE	5	0	0
no. NC AOE	0	2	1
no. NW AOE	1	2	1
no. CW AOE	11	3	2
no. CE AOE	1	1	0
no. SW AOE	9	4	2
no. SE AOE	7	6	3

Table 2. Scaling factors used in coalescent simulations for mtDNA, *RAG* and *RHO*. ($\pi_{between}$ is the average number of substitutions per site between the Sulawesi toads and *Bufo divergens*. The effective population size of mtDNA in each deme is scaled to 0.25 of the size of autosomal DNA (N_e scaling). The mutation rate scaling (μ scaling) is calculated by dividing the $\pi_{between}$ of each locus by the $\pi_{between}$ of *RAG1*. The finite sites scaling factor (FS) is obtained by dividing the number of base pairs of data at the locus by the number of base pairs of data collected for *RAG1*. The product of these scaling factors is the composite θ scaling factor. The time scaling factor is the reciprocal of the N_e scaling factor.)

	mtDNA	*RAG*	*RHO*
base pairs	727	961	338
$\pi_{between}$	0.087	0.015	0.041
N_e scaling	0.25	1.00	1.00
μ scaling	5.929	1.000	2.797
FS	0.757	1.000	0.352
θ scaling	1.1	1.0	1.0
time scaling	4	1	1

differences in uniparental or biparental inheritance, ploidy, mutation rate per nucleotide, and the number of nucleotides sequenced per locus (table 2).

Nested evolutionary models can be compared by assuming that twice the difference of the natural logarithm of their likelihoods of each model (2δ) follows a χ^2 distribution with degrees of freedom equal to the number of free parameters (Goldman 1993). However, because the IBD_L model is equivalent to the IBD_L+F model with τ equal to a boundary of zero, in our case this distribution can be expressed as a 50 : 50 mixture of χ_0^2 and χ_1^2 distributions (Self & Liang 1987). This is equal to half of the probability of a χ^2 distribution with degrees of freedom equal to 1 (Goldman & Whelan 2000).

3. RESULTS

The likelihood of the IBD_L+F model is significantly higher than the likelihood of the IBD_L model when considering all loci ($p=0.0416$), only nuclear loci ($p=0.0269$) or only mtDNA ($p=0.0195$; figure 2; see the electronic supplementary material). When all loci are considered, the 95% confidence interval (CI) of the IBD_L+F model dips below significance. However, this likelihood is compromised by divergent mtDNA lineages in three demes that could be derived from recent gene flow across contact zones (figure 2; see the electronic supplementary material). Support for fragmentation is also apparent in the phylogeography of mtDNA (figure 1) and nuclear DNA (see the electronic supplementary material). Population structure between AOEs is significant at each locus (see the electronic supplementary material). Each AOE has an endemic clade of toad mtDNA, and most have private nuclear alleles in both nuclear loci (table 1).

These new findings support and extend previous work. Notably, the statistical framework reported here incorporates stochasticity of genealogical coalescence. New samples in this study (166 versus 29 samples in Evans *et al.* 2003*c*) demonstrate that contact zones between toad mtDNA clades closely match the locations of macaque hybrid zones (figure 1). In units of $4N_{e\text{-nDNA-deme}}$ generations, the maximum-likelihood time of simultaneous fragmentation is 1.0 when all loci are considered or 2.0 when only nDNA is considered. Using an independent estimate of μ, this time is estimated to be Late Pleistocene (see the electronic supplementary material).

4. DISCUSSION

Using data from up to three loci, rejection sampling of coalescent simulations based on three summary statistics rejects the IBD_L model in favour of the IBD_L+F model. While extensions of the rejection sampling approach, such as approximate Bayesian computation, may improve the accuracy of parameter estimates (Beaumont *et al.* 2002), overall this illustrates, under the assumptions of each model, that population structure in Celebes toads cannot be attributed exclusively to IBD.

Because models simplify real demographic histories, caveats exist in their interpretation. These results do not demonstrate, for example, that the IBD_L+F model is better than other models that we did not consider. Significant improvement over the IBD_L model could also be recovered if not all of these AOEs arose by habitat fragmentation, or if toad AOEs do not precisely match macaque AOEs on a fine geographical scale. However, it is also plausible that more complex scenarios involving multi-taxon fragmentation at the sites of monkey contact zones are significantly better than the ones tested here. These models could include non-simultaneous divergence at different contact zones, fragmentation at some contact zones followed by recent gene flow, and non-simultaneous fragmentation of different sympatric taxa.

Habitat fragmentation of Celebes toads in the same or similar locations as multiple macaque hybrid zones could be a consequence of physical barriers, such as marine inundation in low-lying areas between the SW and WC AOE and between the NW and NC AOE (figure 1), and/or multi-taxon adaptation to substantial ecological transitions between substrate, vegetation and climatic zones (Evans *et al.* 2003*c* and

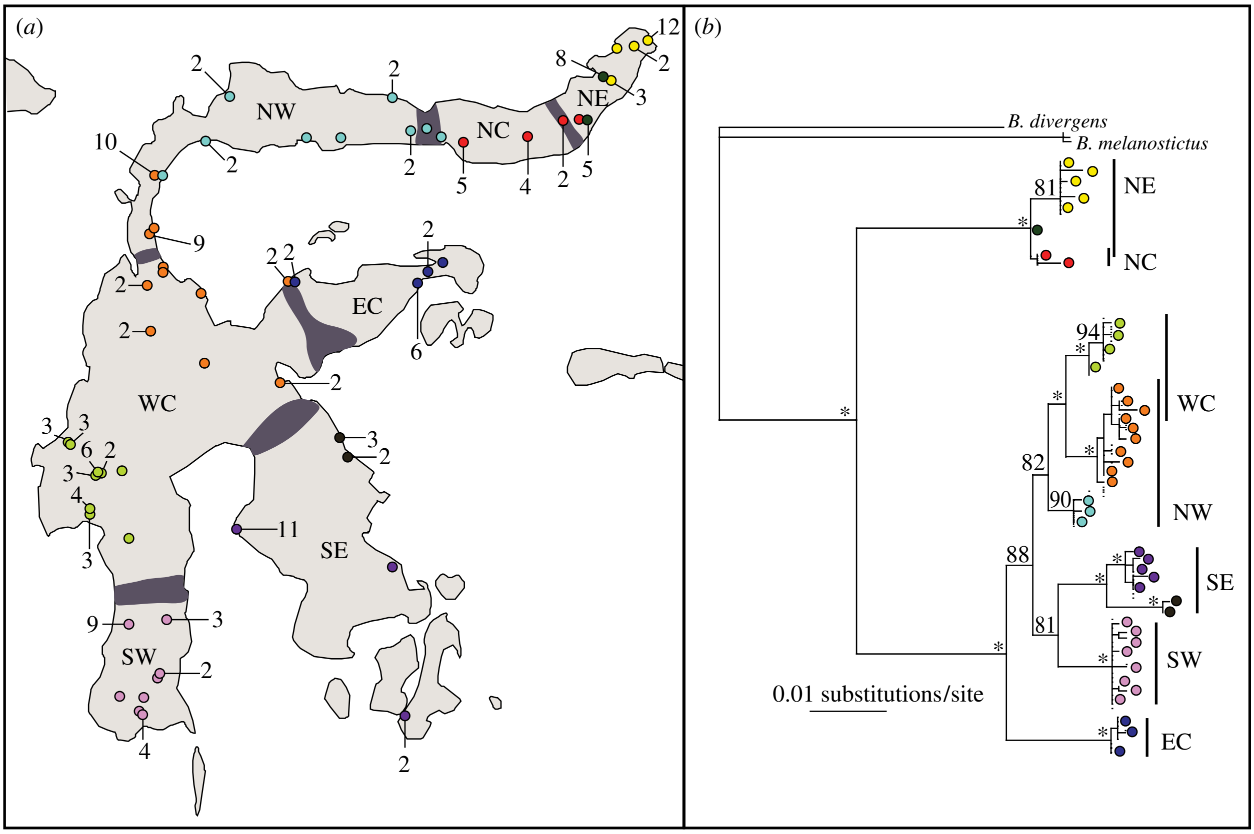

Figure 1. Samples and mtDNA phylogeny of the Celebes toad. (*a*) Sampling localities; the number of individuals sampled at each locality is labelled if more than one. Shaded areas indicate the locations of macaque contact zones. AOEs are labelled: northeast (NE), north-central (NC), northwest (NW), west-central (WC), east-central (EC), southwest (SW) and southeast (SE). (*b*) MtDNA phylogeny of the Celebes toad. Posterior probabilities are above branches; asterisks indicate those above 95%.

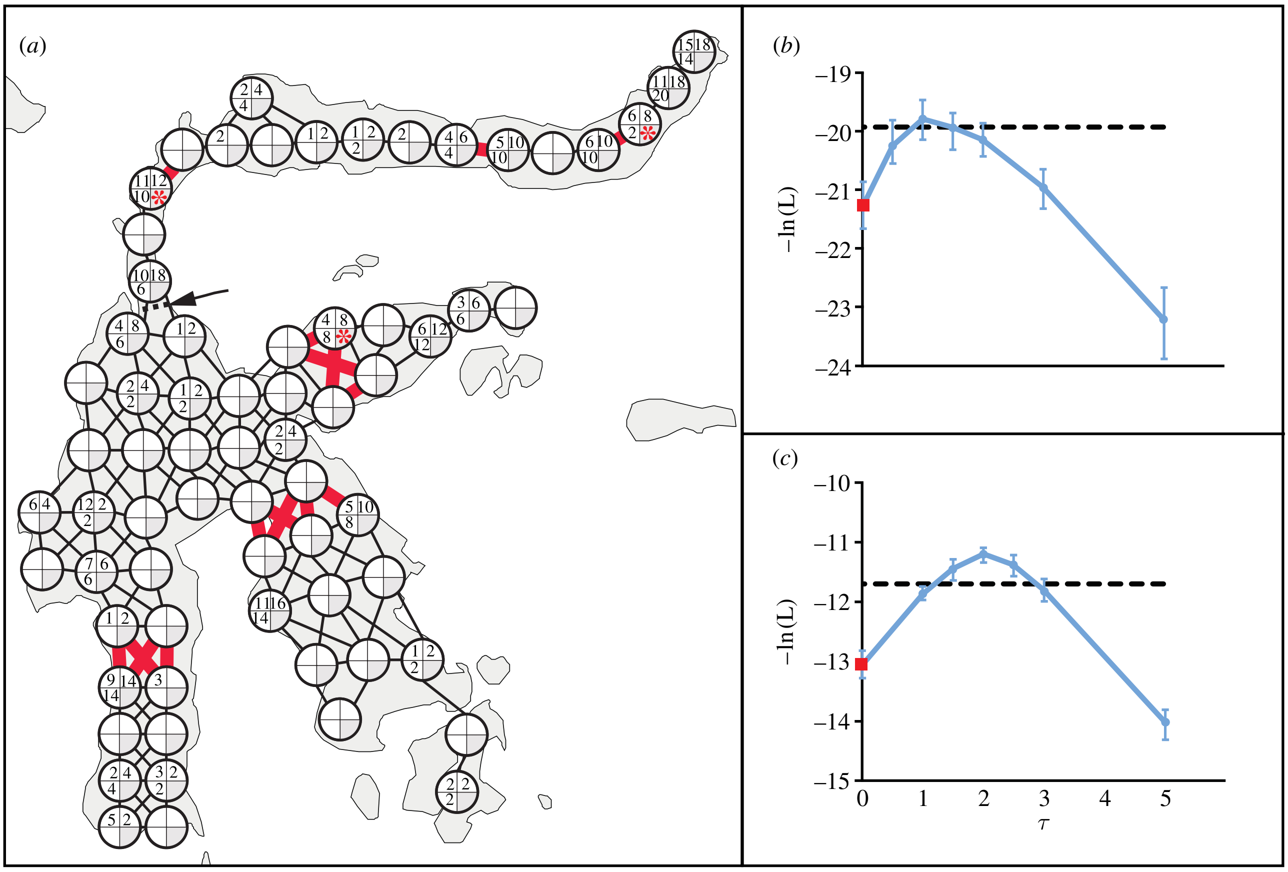

Figure 2. (*Caption opposite*.)

references therein). These processes probably affected many other species and therefore provide scientific rationale for geographically dispersed conservation areas on Sulawesi.

We thank P. Andolfatto, J. Bridle, R. Butlin, B. Golding, N. Goldman, R. Hudson, J. Wilkins and S. Wright and members of the McGuire lab for their advice and comments. This research was supported by the National Science Foundation, Canadian Foundation for Innovation, National Science and Engineering Research Council and McMaster University.

Beaumont, M. A., Zhang, W. & Balding, D. J. 2002 Approximate Bayesian computation in population genetics. *Genetics* **162**, 2025–2035.

Bridle, J. R., Pedro, P. M. & Butlin, R. K. 2004 Habitat fragmentation and biodiversity: testing for the evolutionary effects of refugia. *Evolution* **58**, 1394–1396. (doi:10.1111/j.0014-3820.2004.tb01718.x)

Cannone, J. J. *et al.* 2002 The comparative RNA web (CRW) site: an online database of comparative sequence and structure information for ribosomal, intron, and other RNAs. *BMC Bioinform.* **3**, 2. (doi:10.1186/1471-2105-3-2)

Evans, B. J., Brown, R. M., McGuire, J. A., Supriatna, J., Andayani, N., Diesmos, A., Iskandar, D. T., Melnick, D. J. & Cannatella, D. C. 2003*a* Phylogenetics of fanged frogs (Anura; Ranidae; *Limnonectes*): testing biogeographical hypotheses at the Asian–Australian faunal zone interface. *Syst. Biol.* **52**, 794–819. (doi:10.1080/10635150390251063)

Evans, B. J., Supriatna, J., Andayani, N. & Melnick, D. J. 2003*b* Diversification of Sulawesi macaque monkeys: decoupled evolution of mitochondrial and autosomal DNA. *Evolution* **57**, 1931–1946. (doi:10.1111/j.0014-3820.2003.tb00599.x)

Evans, B. J., Supriatna, J., Andayani, N., Setiadi, M. I., Cannatella, D. C. & Melnick, D. J. 2003*c* Monkeys and toads define areas of endemism on Sulawesi. *Evolution* **57**, 1436–1443. (doi:10.1111/j.0014-3820.2003.tb00350.x)

Glor, R. E., Gifford, M. E., Larson, A., Losos, J. B., Schettino, L. R., Lara, A. R. C. & Jackman, T. R. 2004 Partial island submergence and speciation in an adaptive radiation: a multilocus analysis of the Cuban green anoles. *Proc. R. Soc. B* **271**, 2257–2265. (doi:10.1098/rspb.2004.2819)

Goldman, N. 1993 Statistical tests of models of DNA substitution. *J. Mol. Evol.* **36**, 182–198. (doi:10.1007/BF00166252)

Goldman, N. & Whelan, S. 2000 Statistical tests of gamma-distributed rate heterogeneity in models of sequence evolution in phylogenetics. *Mol. Biol. Evol.* **17**, 975–978.

Hudson, R. R. 2002 Generating samples under a Wright–Fisher neutral model of genetic variation. *Bioinformatics* **18**, 337–338. (doi:10.1093/bioinformatics/18.2.337)

Hudson, R. R., Slatkin, M. & Maddison, W. P. 1992 Estimation of levels of gene flow from DNA sequence data. *Genetics* **132**, 583–589.

Huelsenbeck, J. P. & Ronquist, F. 2001 MrBayes: Bayesian inference of phylogenetic trees. *Bioinformatics* **17**, 754–755. (doi:10.1093/bioinformatics/17.8.754)

Leaché, A., Crews, S. C. & Hickerson, M. J. 2007 Two waves of diversification in mammals and reptiles of Baja California revealed by hierarchical Bayesian analysis. *Biol. Lett.* **3**, 646–650. (doi:10.1098/rsbl.2007.0368)

McGuire, J. A., Brown, R. M., Mumpuni, Riyanto, A. & Andayani, N. 2007 The flying lizards of the *Draco lineatus* group (Squamata: Iguania: Agamidae): a taxonomic revision with descriptions of two new species. *Herpetol. Monogr.* **21**, 179–212. (doi:10.1655/07-012.1)

Rousset, F. 1997 Genetic differentiation and estimation of gene flow from *F*-statistics under isolation by distance. *Genetics* **145**, 1219–1228.

Rozas, J., Sanchez-DelBarrio, J. C., Messegyer, X. & Rozas, R. 2003 DNAsp, DNA polymorphism analyses by the coalescent and other methods. *Bioinformatics* **19**, 2496–2497. (doi:10.1093/bioinformatics/btg359)

Self, S. G. & Liang, K.-Y. 1987 Asymptotic properties of maximum likelihood estimators and likelihood ratio tests under nonstandard conditions. *J. Am. Stat. Assoc.* **82**, 605–610. (doi:10.2307/2289471)

Weiss, G. & von Haeseler, A. 1998 Inference of population history using a likelihood approach. *Genetics* **149**, 1539–1546.

Wilkins, J. F. 2004 A separation-of-timescales approach to the coalescent in a continuous population. *Genetics* **168**, 2227–2244. (doi:10.1534/genetics.103.022830)

Figure 2. (*Opposite.*) Demographic models and likelihoods. (*a*) The $\mathrm{IBD_L}$ and $\mathrm{IBD_L}$+F models consist of 68 demes, represented by circles, some of which exchange migrants, represented by lines between circles. In the $\mathrm{IBD_L}$+F model, no migration occurs between demes connected by red lines from time τ until the present. The number of haplotypes or alleles sampled is indicated inside each deme for mitochondria (top left), *RAG* (top right) and *RHO* (bottom left). An arrow and dashed line indicates the location of a monkey contact zone that is displaced from the margin of toad mtDNA clades. (*b*) Likelihood of the $\mathrm{IBD_L}$+F model as a function of duration of fragmentation (τ) in units of $4N_{\text{e-nDNA-deme}}$ generations, based on mtDNA and nDNA loci, and (*c*) likelihood of the $\mathrm{IBD_L}$+F model based on nDNA loci only. In (*b*,*c*), the likelihood of the $\mathrm{IBD_L}$ model indicated by red squares is equal to that at $\tau=0$. Likelihoods above the dashed line indicate significant improvement of the $\mathrm{IBD_L}$+F model (i.e. that $2\delta>2.7065$). Parameters were calculated to the nearest 0.01 units for Θ ($=4N_e\mu$), the nearest 0.2 for $M_{ij}(=4N_{\text{e-nDNA-deme}}m_{ij})$ and the nearest $2N_{\text{e-nDNA-deme}}$ generations for τ. 95% CIs, indicated as vertical bars, were obtained with 40 replicate simulations. Demes discussed in the electronic supplementary material contain asterisks.

There are five sections to the additional material:

S1. Estimation of divergence time
S2. Supplementary figure 1
S3. Supplementary table 1.
S4. Supplementary table 2.
S5. Supplementary references

S1. Estimation of divergence time

The mutation rate (μ) of mtDNA ribosomal genes has been estimated to be 0.00249 substitutions per site per million years (Evans et al., 2004). This can be scaled to a mutation rate for RAG of 4.20×10^{-10} substitutions per site per year at this locus, based on statistics in Table 2. Because 961 bp of RAG1 sequence were analyzed in this study, this translates to a mutation rate of 4.04×10^{-7} substitutions per RAG sequence per year (μ_{RAG}). Given the relationship $\theta = 4N_{e\text{-nDNA-deme}}\,\mu$, dividing the ML estimate of θ when all loci are considered (0.037) by μ_{RAG}, and assuming one toad generation per year, yields an ML estimate of the estimate of the time of simultaneous fragmentation ($\tau = 1*4N_{e\text{-nDNA-deme}}$ generations) of ~92,000 years ago. Use of the ML estimate of θ when just nDNA are considered (0.044), provides an estimated time of simultaneous fragmentation ($\tau = 2*4N_{e\text{-nDNA-deme}}$ generations) of ~218,000 years ago. Of course, confidence intervals on these estimates are large if one incorporates uncertainty in parameter estimates. For example, consideration of values of τ that are two units of support away from the ML estimate provides a confidence interval analogous to that derived from two standard deviations away from the mean (Edwards, 1992). This interval ranges from 0 to about 340,000 years ago for all loci, and 0 to about 460,000 years ago for just nDNA.

Recent gene flow, which is not incorporated in the IBD_L+F model, probably decreases the multilocus likelihood of this model. For example, in three locations indicated by red asterisks in Fig. 2, two divergent mtDNA lineages were sampled and therefore were included in the same deme for the coalescent simulations. Variation the ML estimate of τ among loci also reduces the multilocus likelihood of the IBD_L+F model: the ML estimate of τ from only mtDNA is older ($4*4N_{e\text{-nDNA-deme}}$ generations, data not shown) than the estimate from the nuclear loci (figure 2). This could be because of inaccuracies in the scaling factors used (Table 2) and/or stochastic variation among loci in coalescent times. But despite these limitations, the IBD_L+F model is still preferred.

Under a scenario of non-simultaneous fragmentation, some contact zones could have experienced fragmentation more recently or not at all, whereas fragmentation at other contact zones could be older than τ. We did not explore these and other more complex demographic models here because of computational difficulty of estimating the maximum likelihood of more parameterized models. Furthermore, additional zones of fragmentation may exist in other species that either do not exist in Sulawesi toads or monkeys, or that are displaced from the ones in these species (Bridle et al., 2001). On a fine geographic scale, then, no single demographic model will account for all species on Sulawesi. It is this reality that makes the similar distributions of genetic variation of toads and monkeys remarkable, and suggestive of cryptic fragmentation that could have impacted diversification of multiple species on this island.

S2. Supplementary figure 1

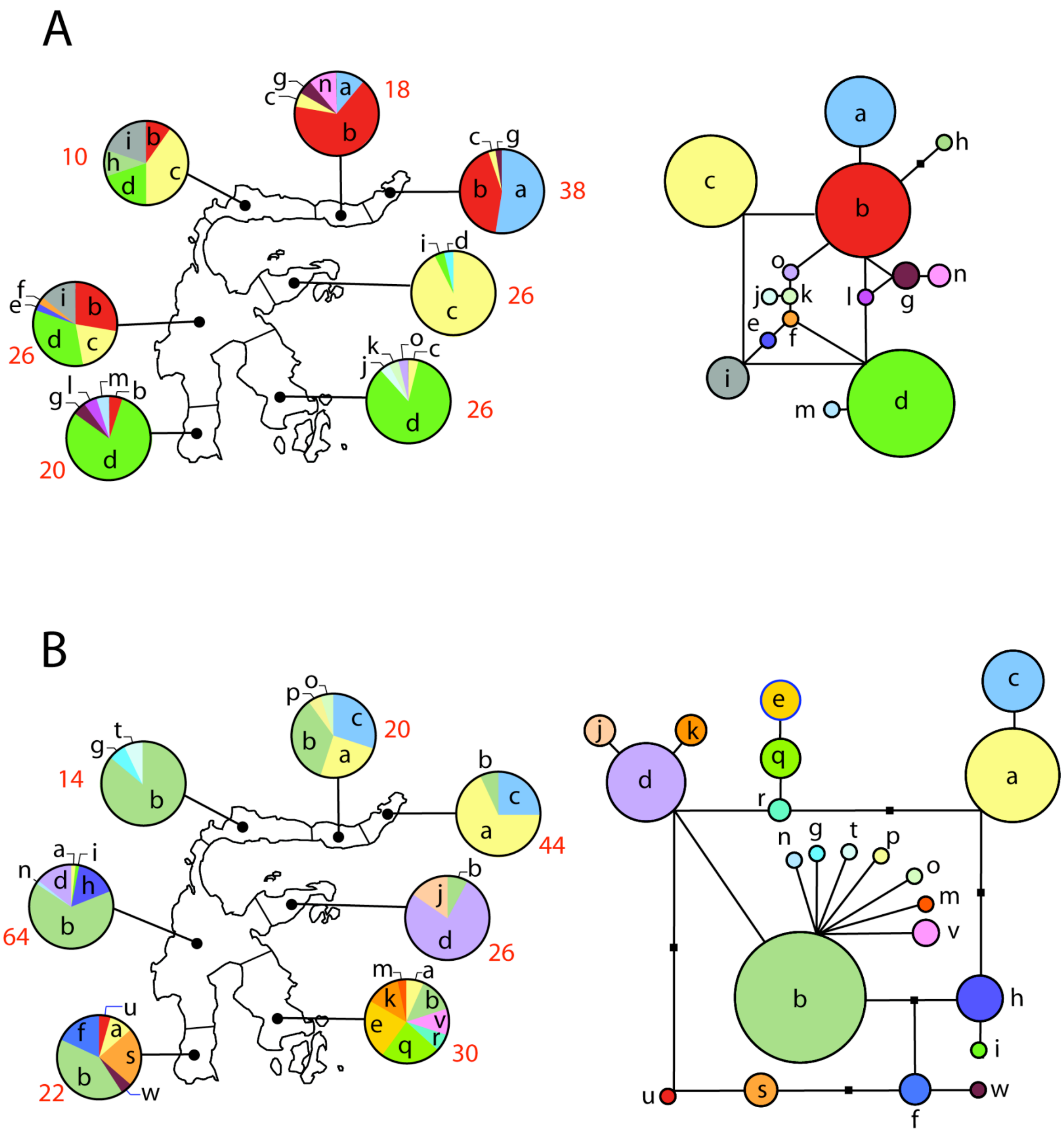

Supplementary figure 1. Allele frequencies and network for two autosomal loci of the Celebes toad, including (A) RHO, and (B) RAG. Red numbers next to each pie chart refer to the number of individual alleles that were sampled in each AOE. In each network, the area of the circle is proportional to the number of alleles that were sampled on Sulawesi and black squares in the network indicate inferred alleles. Sequences of observed nuclear alleles were inferred from unphased diploid genotypes using fastPHASE version 1.2.3 (Scheet & Stephens, 2006) and a statistical parsimony network was constructed from inferred alleles with TCS version 1.18 (Clement et al., 2000).

S3. Supplementary Table 1 (page 1 of 6).

Supplemenary table 1. Sample data for Celebes toad and outgroups. All samples of Celebes toads are from Sulawesi or Buton Island, Indonesia. MtDNA sequences were obtained from all samples; RAG and RHO sequences were obtained from a subset of these samples (+). 12S sequences from mtDNA were obtained using previously published primers (Goebel et al. 1999). Nuclear sequences from RAG and RHO were obtained with new primers: Bufo.Rag1.2611.for (5’ TGG AAG AAA ATA TCC TCG AAG 3’), Bufo.RAG1.3660.rev (5’ TGA TCT TGC CCT CAT ATC TAT AC 3’), Rho3F (5’ TTG ACT ACT ACA CCC TGA AGC 3’), and Rho4R (5’ TGT AGA TGA CGG GAT TGT AGA 3’). These data have been deposited in Genbank (accession numbers AY180213-AY180245, EU712726-EU13068).

Field Number	monkeyAOE	Species	Locality	Latitude	Longitude	RAG	RHO
AMNH16001	Not applicable	*melanostictus*	Java Island, Java Barat, Depok	-6.3739	106.8255	+	+
AMNH16059	SE (introduced)	*melanostictus*	Sulawesi Island, Sulawesi Tengarra, Kendari	-3.9695	122.5733	+	+
AMNH16064	Not applicable	*melanostictus*	Sumatra Island, Sumatra Barat, Padang	-0.9500	100.3500	+	+
AMNH16179	Not applicable	*divergens*	Borneo Island, Kalimantan Timor, Kutai National Park	0.3696	117.4730	+	+
AMNH16002	NE	*celebensis*	Manado	1.4897	124.8420	+	+
AMNH16008	NE	*celebensis*	Tangkoko N. P.	1.5701	125.1569	+	+
AMNH16009	NE	*celebensis*	Tangkoko N. P.	1.5701	125.1569	+	+
AMNH16010	NE	*celebensis*	Tangkoko N. P.	1.5701	125.1569	+	+
AMNH16011	NE	*celebensis*	Tangkoko N. P.	1.5701	125.1569	+	+
AMNH16018	NC	*celebensis*	Kotamobagu	0.7292	124.2830	+	+
AMNH16023	NC	*celebensis*	Toraut, Bogani Nani Wartabone N. P.	0.5625	123.9038	+	+
AMNH16028	NC	*celebensis*	Toraut, Bogani Nani Wartabone N. P.	0.5625	123.9038	+	+
AMNH16041	WC	*celebensis*	Lore Lindu N.P.	-1.4503	119.9899	+	+
AMNH16048	WC	*celebensis*	Kolonodale	-1.9866	121.3390	+	+
AMNH16056	SE	*celebensis*	Kendari, Soropia	-3.9072	122.5046	+	+
AMNH16068	SW	*celebensis*	Malino	-5.2594	119.9260	+	+
AMNH16069	SW	*celebensis*	Bantimurung	-5.2520	119.6730	+	+
AMNH16082	WC	*celebensis*	Gunung Karua	-2.9022	119.6973	+	+
AMNH16091	EC	*celebensis*	Luwuk	-0.9509	122.7916	+	+
AMNH16133	WC	*celebensis*	Parigi	-0.7884	120.1270	+	+
AMNH16137	WC	*celebensis*	Lemo	-0.4408	119.9820	+	+
AMNH16146	NW	*celebensis*	Marisa	0.5516	121.9690	+	+
AMNH16147	NW	*celebensis*	Paguyaman	0.6291	122.6927	+	+
AMNH16150	NC	*celebensis*	Tolabulu	0.5134	123.2428	+	+
AMNH16151	NE	*celebensis*	Mooat	0.7515	124.4492	+	+
AMNH16154	SE	*celebensis*	Buton Island	-5.4502	122.6419	+	+
AMNH16163	SE	*celebensis*	Lasusua	-3.5101	120.8819		+
AMNH16169	WC	*celebensis*	Enrekang	-3.6024	119.7664	+	
AMNH16173	SW	*celebensis*	Barru	-4.4941	119.7666	+	+
BSI0119	NE	*celebensis*	Klabat Mt.	1.5097	125.0183	+	+
BSI0135	NE	*celebensis*	Klabat Mt.	1.5111	125.0178	+	+
BSI0140	NE	*celebensis*	Soputan, Kabupaten Minahasa, Sulawesi Utara Prov	1.1447	124.7556	+	+
BSI0141	NE	*celebensis*	Soputan	1.1447	124.7556	+	+
BSI0142	NE	*celebensis*	Soputan	1.1447	124.7556	+	+
BSI0143	NE	*celebensis*	Soputan	1.1447	124.7556	+	+
BSI0144	NE	*celebensis*	Soputan, Kabupaten Minahasa, Sulawesi Utara Prov	1.1447	124.7556	+	+
BSI0145	NE	*celebensis*	Soputan, Kabupaten Minahasa, Sulawesi Utara Prov	1.1447	124.7556	+	+
BSI0148	NE	*celebensis*	Soputan, Kabupaten Minahasa, Sulawesi Utara Prov	1.1447	124.7556	+	+
BSI0150	NE	*celebensis*	Soputan, Kabupaten Minahasa, Sulawesi Utara Prov	1.1447	124.7556		+
BSI0151	NE	*celebensis*	Soputan, Kabupaten Minahasa, Sulawesi Utara Prov	1.1447	124.7556	+	+
BSI0152	NE	*celebensis*	Soputan	1.1483	124.7789		
BSI0153	NE	*celebensis*	Soputan	1.1483	124.7789	+	+
BSI0748	NW	*celebensis*	Desa Buladu, Kabupaten Gorontalo, Gorontalo Prov	0.9759	122.5058		

S3. Supplementary Table 1 (page 2 of 6).

BSI0844	NW	*celebensis*	Desa Buladu, Kabupaten Gorontalo, Gorontalo Prov	0.9687	122.5052		
BSI0908	NW	*celebensis*	Desa Mulionegoro, Kabupaten Limboto, Gorontalo Prov	0.6297	122.6954	+	+
BSI0928	NW	*celebensis*	Desa Isimu, Kabupaten Gorontalo, Gorontalo Prov	0.6486	122.8675		
BSI1105	NW	*celebensis*	Desa Wonggarasi, Kabupaten Pohuwatu, Gorontalo Prov	0.5606	121.6084	+	
BSI1147	NW	*celebensis*	Marantale, Sulawesi Tengah	0.5353	122.9801	+	
BSI1151	NW	*celebensis*	Desa Ogotomubu, Kabupaten Parigi-Mouotong, Sulawesi Tengah Prov	0.5153	120.5687		
BSI1152	NW	*celebensis*	Desa Ogotomubu, Kabupaten Parigi-Mouotong, Sulawesi Tengah Prov	0.5153	120.5687		
BSI1182	NW	*celebensis*	Desa Sipayo, Kabupaten Parigi-Moutong, Sulawesi Tengah Prov	0.1914	120.1307	+	+
BSI1183	NW	*celebensis*	Desa Sipayo, Kabupaten Parigi-Moutong, Sulawesi Tengah Prov	0.1914	120.1307	+	+
BSI1184	NW	*celebensis*	Desa Sipayo, Kabupaten Parigi-Moutong, Sulawesi Tengah Prov	0.1914	120.1307	+	+
BSI1185	NW	*celebensis*	Desa Sipayo, Kabupaten Parigi-Moutong, Sulawesi Tengah Prov	0.1914	120.1307	+	+
BSI1186	NW	*celebensis*	Desa Sipayo, Kabupaten Parigi-Moutong, Sulawesi Tengah Prov	0.1914	120.1307	+	
BSI1187	NW	*celebensis*	Desa Sipayo, Kabupaten Parigi-Moutong, Sulawesi	0.1914	120.1307		
BSI1188	NW	*celebensis*	Parigi-Moutong, Sulawesi Tengah Prov	0.1914	120.1307		
BSI1189	NW	*celebensis*	Desa Sipayo, Kabupaten Parigi-Moutong, Sulawesi Tengah Prov	0.1914	120.1307		
BSI1190	NW	*celebensis*	Desa Sipayo, Kabupaten Parigi-Moutong, Sulawesi Tengah Prov	0.1914	120.1307		
BSI1191	NW	*celebensis*	Desa Sipayo, Kabupaten Parigi-Moutong, Sulawesi Tengah Prov	0.1914	120.1307		
BSI1192	NW	*celebensis*	Desa Sipayo, Kabupaten Parigi-Moutong, Sulawesi Tengah Prov	0.1914	120.1307	+	+
BSI1198	WC	*celebensis*	Tomoli	-0.3803	120.0337	+	+
BSI2428	WC	*celebensis*	Desa Keang, Kabupaten Mamuju, Sulawesi Barat Prov	-2.6246	119.1472	+	
BSI2429	WC	*celebensis*	Desa Keang, Kabupaten Mamuju, Sulawesi Barat Prov	-2.6246	119.1472	+	

S3. Supplementary Table 1 (page 3 of 6).

BSI2586	WC	*celebensis*	Desa Kelapa Dua, Kabupaten Polewali, Sulawesi Barat Prov.	-3.3615	119.3607	+	+
BSI2587	WC	*celebensis*	Desa Kelapa Dua, Kabupaten Polewali, Sulawesi Barat Prov.	-3.3615	119.3607	+	+
BSI2589	WC	*celebensis*	Desa Kelapa Dua, Kabupaten Polewali, Sulawesi Barat Prov.	-3.3458	119.3658	+	+
BSI2658	SW	*celebensis*	Desa Kamilo, Kabupaten Bone, Sulawesi Selatan Prov	-5.0318	120.0682		
BSI2659	SW	*celebensis*	Desa Kamilo, Kabupaten Bone, Sulawesi Selatan Prov	-5.0148	120.0957	+	
BSI2662	SW	*celebensis*	Desa Kamilo, Kabupaten Bone, Sulawesi Selatan Prov	-5.0148	120.0957		
JAM3668	EC	*celebensis*	Propinsi Sulawesi Tengah, Kabupaten Banggai, Kecamatan Luwuk, Kota Luwuk, Air Terjun Hengahenga	-0.9582	122.7722	+	+
JAM3669	EC	*celebensis*	Propinsi Sulawesi Tengah, Kabupaten Banggai, Kecamatan Luwuk, Kota Luwuk, Air Terjun Hengahenga	-0.9582	122.7722	+	+
JAM3670	EC	*celebensis*	Propinsi Sulawesi Tengah, Kabupaten Banggai, Kecamatan Luwuk, Kota Luwuk, Air Terjun Hengahenga	-0.9582	122.7722	+	+
JAM3671	EC	*celebensis*	Propinsi Sulawesi Tengah, Kabupaten Banggai, Kecamatan Luwuk, Kota Luwuk, Air Terjun Hengahenga	-0.9582	122.7722	+	+
JAM3711	EC	*celebensis*	Propinsi Sulawesi Tengah, Kabupaten Banggai, Kecamatan Luwuk, Desa Salodik	-0.8307	122.8698	+	+
JAM3712	EC	*celebensis*	Propinsi Sulawesi Tengah, Kabupaten Banggai, Kecamatan Luwuk, Desa Salodik	-0.8307	122.8698	+	+
JAM3955	EC	*celebensis*	Propinsi Sulawesi Tengah, Kabupaten Banggai,	-0.9582	122.7722	+	+
JAM4903	WC	*celebensis*	Biromaro, Sulawesi Tengah Prov.	-0.9751	119.9613	+	+
JAM4904	WC	*celebensis*	Desa Pombewe, Kec. Sigi Biromaro, Sulawesi Tengah Prov.	-0.9751	119.9613	+	+
JAM4915	WC	*celebensis*	Desa Paringinpu, Kabupaten Parigi-Moutong, Sulawesi Tengah Prov	-0.8157	120.1196	+	
JAM4992	SE	*celebensis*	Desa Bungku, Kabupaten Parigi-Moutong, Sulawesi Tengah Prov	-2.5600	121.9574	+	
JAM4993	SE	*celebensis*	Desa Bungku, Kabupaten Parigi-Moutong, Sulawesi Tengah Prov	-2.5600	121.9574	+	+
JAM4994	SE	*celebensis*	Desa Bungku, Kabupaten Parigi-Moutong, Sulawesi Tengah Prov	-2.5600	121.9574	+	+

S3. Supplementary Table 1 (page 4 of 6).

JAM5005	SE	*celebensis*	Desa Dampala, Kabupaten Parigi-Moutong	-2.7626	122.0368	+	+
JAM5006	SE	*celebensis*	Desa Dampala, Kabupaten Parigi-Moutong	-2.7626	122.0368	+	+
JAM5065	WC	*celebensis*	Desa Korowau, Sulawesi Tengah Prov	-1.7869	120.5544	+	+
JAM5104	WC	*celebensis*	Desa Maleali, Kecamatan Sausu, Kabupaten Parigi-Moutong, Sulawesi Tengah Prov	-1.0586	120.5237	+	
JAM5465	SW	*celebensis*	Desa Bontomaranu, Kecematan Uluere, Kabupaten Bataeng Loka, Sulawesi Selatan Prov	-5.4405	119.9152		
JAM5467	SW	*celebensis*	Desa Bontomaranu, Kecematan Uluere, Kabupaten Bataeng Loka, Sulawesi Selatan Prov	-5.4405	119.9152		
JAM5468	SW	*celebensis*	Desa Bontomaranu, Kecematan Uluere, Kabupaten Bataeng Loka, Sulawesi Selatan Prov	-5.4405	119.9152		
JAM5469	SW	*celebensis*	Desa Bontomaranu, Kecematan Uluere, Kabupaten Bataeng Loka, Sulawesi Selatan Prov	-5.4405	119.9152		
JAM5859	SW	*celebensis*	Desa Pecinong, Sungai Kasingpang, Sulawesi Sulatan Prov	-4.4515	120.1600		
JAM5860	SW	*celebensis*	Desa Pecinong, Sungai Kasingpang, Sulawesi Sulatan Prov	-4.4515	120.1600		
JAM5861	SW	*celebensis*	Desa Pecinong, Sungai Kasingpang, Sulawesi Sulatan Prov	-4.4515	120.1600		
JAM5955	WC	*celebensis*	Polewali Masawa Road, Kec. Messawa, Kab. Polman, Desa Makuang, Sulawesi Barat	-3.3154	119.3725		
JAM6006	WC	*celebensis*	Polewali Masawa Road, Kec. Messawa, Kab.	-3.2990	119.3701		
JAM6007	WC	*celebensis*	Kec. Messawa, Kab. Polman, Desa Makuang,	-3.2990	119.3701		
JAM6008	WC	*celebensis*	Polewali Masawa Road, Kec. Messawa, Kab. Polman, Desa Makuang, Sulawesi Barat	-3.2990	119.3701		
JAM6046	WC	*celebensis*	Desa Lambangan, Kecematan Mamasa, Kabupaten Mamasa, Sulawesi Barat Prov	-2.9244	119.4698		
JAM6047	WC	*celebensis*	Desa Lambangan, Kecematan Mamasa, Kabupaten Mamasa, Sulawesi Barat Prov	-2.9244	119.4698		
JAM6048	WC	*celebensis*	Desa Lambangan, Kecematan Mamasa, Kabupaten Mamasa, Sulawesi Barat Prov	-2.9244	119.4698		

S3. Supplementary Table 1 (page 5 of 6).

JAM6110	WC	*celebensis*	Desa Lambangan, Kecematan Mamasa, Kabupaten Mamasa, Sulawesi Barat Prov	-2.9244	119.4698		
JAM6157	WC	*celebensis*	Desa Lambangan, Kecematan Mamasa, Kabupaten Mamasa, Sulawesi Barat Prov	-2.9244	119.4698		
JAM6158	WC	*celebensis*	Desa Lambangan, Kecematan Mamasa, Kabupaten Mamasa, Sulawesi Barat Prov	-2.9244	119.4698		
JAM6159	WC	*celebensis*	Desa Lambangan, Kecematan Mamasa, Kabupaten Mamasa, Sulawesi Barat Prov	-2.9244	119.4698		
JAM6167	WC	*celebensis*	Desa Tadok, Kecematan Tabang, Kabupaten Mamasa, Sulawesi Barat Prov	-2.9247	119.4814		
JAM6199	WC	*celebensis*	Trail to waterfall ~7km NE Mamasa, Kecematan Mamasa, Kabupaten Mamasa, Sulawesi Barat Prov	-2.9504	119.4192		
JAM6537	WC	*celebensis*	Tasiu-Tibo Road, Kabupaten Mamuju, Sulawesi Barat Prov	-2.9504	119.4192		
JAM6545	WC	*celebensis*	Tasiu-Tibo Road, Kabupaten Mamuju, Sulawesi Barat Prov	-2.9504	119.4192		
JAM6546	WC	*celebensis*	Tasiu-Tibo Road, Kabupaten Mamuju, Sulawesi Barat Prov	-2.6114	119.1443		
JAM6600	WC	*celebensis*	Desa Kaeng, Kabupaten Mamuju, Sulawesi Barat Prov	-2.6321	119.1582		
JAM6601	WC	*celebensis*	Desa Kaeng, Kabupaten Mamuju, Sulawesi Barat Prov	-2.6321	119.1582		
JAM6602	WC	*celebensis*	Desa Kaeng, Kabupaten Mamuju, Sulawesi Barat Prov	-2.6321	119.1582		
RMB1235	SW	*celebensis*	Mt. Lompobattang, Sulawesi Selatan	-5.4000	119.9000	+	+
RMB1443	EC	*celebensis*	Marawo, Sulawesi Tengah	-0.9492	121.4517	+	+
RMB1447	EC	*celebensis*	Marawo, Sulawesi Tengah	-0.9492	121.4517	+	+
RMB1480	EC	*celebensis*	Marawo, Sulawesi Tengah	-0.9492	121.4517	+	+
RMB1564	EC	*celebensis*	Marawo, Sulawesi Tengah	-0.9492	121.4517	+	+
RMB1682	EC	*celebensis*	Siuna, Sulawesi Tengah	-0.7446	123.0335	+	+
RMB4631	NW	*celebensis*	Desa Dadakitan, Kecamatan Baolan, Kabupaten Toli-toli, Sulawesi Tengah Prov	0.9792	120.8175	+	+
RMB4632	NW	*celebensis*	Desa Dadakitan, Kecamatan Baolan, Kabupaten Toli-toli, Sulawesi Tengah Prov	0.9792	120.8175	+	+
UI0001	NE	*celebensis*	Tangkoko N. P.	1.5700	125.1570		
UI0006	NE	*celebensis*	Tangkoko N. P.	1.5701	125.1569		
UI0011	NC	*celebensis*	Kotamobagu	0.7292	124.2830		
UI0013	NC	*celebensis*	Toraut, Bogani Nani Wartabone N. P.	0.5625	123.9038	+	+
UI0014	NC	*celebensis*	Toraut, Bogani Nani Wartabone N. P.	0.5625	123.9038	+	+
UI0051	WC	*celebensis*	Desa Matawe, Kec. Kulaui, Lore Lindu N. P.	-1.4503	119.9899	+	
UI0064	WC	*celebensis*	Kolonodale	-1.9866	121.3390	+	
UI1114	NE	*celebensis*	Tangkoko N. P.	1.5701	125.1569	+	
UI1118	NE	*celebensis*	Tangkoko N. P.	1.5701	125.1569		
UI1121	NE	*celebensis*	Tangkoko N. P.	1.5701	125.1569		
UI1122	NE	*celebensis*	Tangkoko N. P.	1.5701	125.1569		
UI1123	NE	*celebensis*	Tangkoko N. P.	1.5701	125.1569		

S3. Supplementary Table 1 (page 6 of 6).

UI1136	WC	*celebensis*	Lemo	-0.4408	119.9830	+	
UI1138	WC	*celebensis*	Lemo	-0.4408	119.9830	+	
UI1139	WC	*celebensis*	Lemo	-0.4408	119.9830	+	
UI1140	WC	*celebensis*	Lemo	-0.4408	119.9830	+	
UI1141	WC	*celebensis*	Lemo	-0.4408	119.9830		
UI1142	WC	*celebensis*	Lemo	-0.4408	119.9830	+	
UI1143	WC	*celebensis*	Lemo	-0.4408	119.9830	+	
UI1144	WC	*celebensis*	Lemo	-0.4408	119.9830	+	+
UI1157	NC	*celebensis*	Tulabolo, 20 km east of Gorontalo	0.5134	123.2428	+	+
UI1158	NC	*celebensis*	Tulabolo, 20 km east of Gorontalo	0.5134	123.2428	+	+
UI1159	NC	*celebensis*	Tulabolo, 20 km east of Gorontalo	0.5134	123.2428	+	+
UI1160	NC	*celebensis*	Tulabolo, 20 km east of Gorontalo	0.5134	123.2428	+	+
UI1162	NE	*celebensis*	Mooat	0.7515	124.4492		
UI1163	NE	*celebensis*	Mooat	0.7515	124.4492	+	
UI1164	NE	*celebensis*	Mooat	0.7515	124.4492	+	
UI1165	NE	*celebensis*	Mooat	0.7515	124.4492	+	
UI1166	NE	*celebensis*	Mooat	0.7515	124.4492		
UI1174	SE	*celebensis*	Buton Island	-5.4502	122.6419		
UI1181	SE	*celebensis*	Lasusua	-3.5101	120.8819	+	+
UI1182	SE	*celebensis*	Lasusua	-3.5101	120.8819	+	+
UI1183	SE	*celebensis*	Lasusua	-3.5101	120.8819	+	+
UI1184	SE	*celebensis*	Lasusua	-3.5101	120.8819	+	+
UI1185	SE	*celebensis*	Lasusua	-3.5101	120.8819		+
UI1186	SE	*celebensis*	Lasusua	-3.5101	120.8819	+	+
UI1187	SE	*celebensis*	Lasusua	-3.5101	120.8819		
UI1188	SE	*celebensis*	Lasusua	-3.5101	120.8819	+	
UI1190	SE	*celebensis*	Lasusua	-3.5101	120.8819	+	
UI1191	SE	*celebensis*	Lasusua	-3.5101	120.8819	+	
UI1206	SW	*celebensis*	Barrru	-4.4941	119.7666	+	+
UI1207	SW	*celebensis*	Barrru	-4.4941	119.7666	+	+
UI1208	SW	*celebensis*	Barrru	-4.4941	119.7666	+	+
UI1211	SW	*celebensis*	Barrru	-4.4941	119.7666	+	+
UI1212	SW	*celebensis*	Barrru	-4.4941	119.7666		+
UI1213	SW	*celebensis*	Barrru	-4.4941	119.7666	+	+
UI1214	SW	*celebensis*	Barrru	-4.4941	119.7666		
UI1215	SW	*celebensis*	Barrru	-4.4941	119.7666	+	

S4. Supplementary Table 2

Supplementary table 2. Per locus F_{ST} of pairwise comparisons between populations of the Celebes toad. The first diagonal matrix is based on mtDNA. Below the diagonal of this matrix is RHO, and above the diagonal of the second matrix is RAG. Except where indicated by an asterisk, all values are significantly greater than zero after Bonferroni correction for 21 comparisons per locus. AOEs are abbreviated with two letter symbols as in Fig. 1. Pairwise F_{ST} was calculated based on pairwise genetic distances using Arlequin version 3.1 (Excoffier et al. 2005), and departure from the null hypothesis of no differentiation was assessed using 1,000 permutations.

	MtDNA						
	NE	NC	NW	CW	CE	SW	SE
NE	-						
NC	0.50131	-					
NW	0.88768	0.85921	-				
CW	0.81706	0.79392	0.33052	-			
CE	0.92242	0.92091	0.62599	0.52121	-		
SW	0.95728	0.98035	0.67503	0.59241	0.86597	-	
SE	0.92764	0.92818	0.64889	0.5322	0.74396	0.8087	-

	RHO\RAG						
	NE	NC	NW	CW	CE	SW	SE
NE	-	0.2688	0.8220	0.7282	0.7863	0.6022	0.5563
NC	0.1688	-	0.4109	0.3482	0.4380	0.1737	0.2370
NW	0.4803	0.3083	-	0.0704	0.6988	0.1909	0.3898
CW	0.4299	0.2828	0.01815*	-	0.4391	0.1237	0.4050
CE	0.7140	0.6424	0.2815	0.4256	-	0.3453	0.3007
SW	0.6523	0.5560	0.4225	0.2218	0.8271	-	0.2663
SE	0.6610	0.5793	0.4269	0.2267	0.8095	0.01431*	-

S5. References

Bridle, J. R., Garn, A., Monk, K. A. & Butlin, R. K. 2001 Speciation in *Chitaura* grasshoppers (Acrididae: Oxyinae) on the island of Sulawesi: colour patterns, morphology and contact zones. *Biol. J. Linn. Soc.* 72, 373-390.

Clement, M., Posada, D. & Crandall, K. A. 2000 TCS: a computer program to estimate gene genealogies. *Mol. Ecol.* 9, 257-270.

Edwards, A. W. F. 1992 *Likelihood expanded edition* Baltimore: The Johns Hopkins Press.

Evans, B. J., Kelley, D. B., Tinsley, R. C., Melnick, D. J. & Cannatella, D. C. 2004 A mitochondrial DNA phylogeny of clawed frogs: phylogeography on sub-Saharan Africa and implications for polyploid evolution. *Mol. Phylogenet. Evol.* 33, 197-213.

Excoffier, L., Laval, G. & Schneider, S. 2005 Arlequin ver. 3.0: an integrated software package for population genetics data analysis. *Evolutionary Bioinformatics Online* 1, 47-50.

Goebel, A. M., Donnelley, J. M. & Atz, M. E. 1999 PCR primers and amplification methods for 12S ribosomal DNA, the control region, cytochrome oxidase I, and cytochrome *b* in bufonids and other frogs, and an overview of PCR primers which have amplified DNA in amphibians successfully. *Mol. Phylogenet. Evol.* 11, 163-199.

Scheet, P. & Stephens, M. 2006 A fast and flexible statistical model for large-scale population genotype data: Applications to inferring missing genotypes and haplotypic phase. *Am. J. Hum. Gen.* 78, 629-644.